

# Electrocatalytic oxygen reduction reaction promoted by titanium-based tetrapyrazinoporphyrazines

Fabrizio Sordello<sup>1</sup> | Pelagia-Nefeli Prantsidou-Georgiadou<sup>1</sup> |  
Emanuele Azzi<sup>1</sup> | Yannick Tschauder<sup>2,3</sup> | Dario Formenti<sup>3</sup> |  
Francesco Pellegrino<sup>1</sup> | Polyssena Renzi<sup>1</sup>

<sup>1</sup>Department of Chemistry, University of Turin, Turin, Italy

<sup>2</sup>Chemical Process Engineering AVT.CVT, RWTH Aachen University, Aachen, Germany

<sup>3</sup>Institute of Inorganic Chemistry, RWTH Aachen University, Aachen, Germany

## Correspondence

Polyssena Renzi and Fabrizio Sordello, Department of Chemistry, University of Turin, Via Pietro Giuria, 7, 10125 Turin, Italy.

Email: [polyssena.renzi@unito.it](mailto:polyssena.renzi@unito.it) and [fabrizio.sordello@unito.it](mailto:fabrizio.sordello@unito.it)

## Funding information

Fondazione Cassa Di Risparmio Di Torino, Grant/Award Number: 2021. AI717.U809/RF=2021.0684

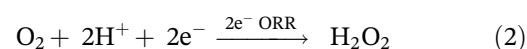
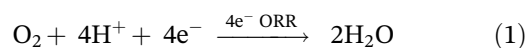
In this study, we unveiled titanium-based tetrapyrazinoporphyrazines as a valuable alternative to noble metals in the oxygen reduction reaction (ORR). By simply modifying the synthetic conditions, we were able to tune the ORR selectivity while showing that the introduction of substituents on the macrocycle periphery is detrimental to the ability of the complex to reduce molecular oxygen. A complete electrochemical characterization in different conditions is reported together with rotating ring-disk electrode measurements, which assessed the possibility of selectively switching from 2- to a 4-electron reduction product changing the titanium precursor amounts during the complex synthesis.

## KEYWORDS

cyclic voltammetry, macrocycles, oxygen reduction reaction, tetrapyrazinoporphyrazines, titanium

## 1 | INTRODUCTION

Over the last decades, the development of alternative energy technologies to cope with the climate change and the rise of energy prices has become increasingly important, particularly in those areas where industrialization is predominant. In this context, fuel cells may represent a valuable tool for obtaining green electricity directly from hydrogen (H<sub>2</sub>) and oxygen (O<sub>2</sub>) with potentially zero environmental impact. In fact, the net reaction happening in the cell is the combination of H<sub>2</sub> and O<sub>2</sub> to generate electricity and, as the only waste products, water (H<sub>2</sub>O) or hydrogen peroxide (H<sub>2</sub>O<sub>2</sub>) depending on the number of electrons exchanged (Equations (1) and (2)).



Despite a lot of attention has been paid to the development of efficient catalysts for the reduction of O<sub>2</sub> to H<sub>2</sub>O, nowadays, a potential sustainable production of H<sub>2</sub>O<sub>2</sub> is also regarded as a valuable process.<sup>1</sup> Founding applications in wastewater purification<sup>2</sup> and chemical industry and paper bleaching,<sup>3</sup> H<sub>2</sub>O<sub>2</sub> is among the most utilized 100 chemical compounds in the world.<sup>4</sup> Its industry is appraised to reach \$6 billion by 2023 with an annual production superior to 4 million tons per year.<sup>5</sup>

This is an open access article under the terms of the [Creative Commons Attribution](#) License, which permits use, distribution and reproduction in any medium, provided the original work is properly cited.

© 2023 The Authors. *Applied Organometallic Chemistry* published by John Wiley & Sons Ltd.

Therefore, the search for stable and low-cost catalytic systems able to perform a selective and green 2-electron  $O_2$  reduction reaction (ORR)<sup>6</sup> is of fundamental importance allowing for decentralized  $H_2O_2$  production in alternative to the well-established anthraquinone oxidation process.<sup>7</sup> In acidic media, the 2-electron ORR is generally catalyzed by alloys composed of expensive and often toxic metals (Pd-Hg, Pt-Hg and Au).<sup>8</sup> However, the need for sustainable and greener production conditions imposes to look for alternative non-noble metal electrocatalysts.<sup>9</sup> In the last years, this lack has been partially filled by metal-containing macrocycles especially in the form of heterogeneous catalysts showing an improved stability.<sup>10</sup> Starting from the first report of Jasinski in 1964,<sup>11</sup> porphyrins, corroles and phthalocyanines were revealed to be excellent ORR catalysts, above all for the 4-electron pathway leading to  $H_2O$  in both acidic and alkaline media, giving in some cases results that are comparable with those of platinum catalysts.<sup>12</sup> Only very recently, Li et al. disclosed, by high-throughput computational screening, a highly selective cobalt porphyrin enabling  $H_2O_2$  production in acid conditions with an onset potential of nearly 0.68 V,  $H_2O_2$  selectivity >90% and stability over a wide range of potentials.<sup>13</sup>

In general, the performances of these macrocycles are linked to their ability to complex a variety of transition metals providing a stable coordination environment not only for the metal but also for  $O_2$  and the high-valent metal ions, which are believed to be involved as key intermediates in  $O_2$  reduction.<sup>12a</sup> Their back-bones can be systematically modified with different functional moieties tuning in this way the catalytic activity.<sup>14</sup> Moreover, the redox chemistry of the metal complex can be modulated by the redox non-innocence of the macrocyclic ligand itself. Although porphyrin, corrole and phthalocyanine-based ligands show high performances, their synthesis is frequently characterized by low yields, a feature that can hamper their production on industrial scale. A valid alternative is represented by tetrapyrzino-porphyrazines (TPyzPzs), the aza-analogues of phthalocyanines. These macrocycles have found application in different fields ranging from electronic components and electrochemical devices, to pigments, photoactivators and catalysts.<sup>15</sup>

Concerning the application of TPyzPzs as ORR catalysts, the field is still in its infancy. Only simple structures have been tested showing promising results for a selective 4-electron ORR, when Fe (II), Co (II) or Zr (IV) TPyzPz complexes are adsorbed onto glassy carbon electrodes or supported on multiwalled carbon nanotubes.<sup>16</sup> Therefore, these compounds represent a good starting point to systematically explore their applicability in the ORR process. In this work, we present titanium-based

complexes of tetrakis-2,3-[5,6-di- $R_8$ -pyrazino]porphyrazine ( $R = H, 2-Py, Ph, 4-MeOPh, 4-BrPh$ ) as ORR electrocatalysts. Interestingly, we were able to tune the ORR selectivity towards  $H_2O_2$  or  $H_2O$  simply by modifying the amount of titanium (IV) butoxide ( $Ti(OBu)_4$ ) employed in the synthesis of the complex.

## 2 | EXPERIMENTAL

### 2.1 | Preparative aspects

As reported in the Experimental section (see Figures S4–S22), ligands **2a–e** and complexes **3a–e** and **4a** can be prepared from the common starting-materials **1a–e** (Scheme 1 and Figures S7–S22). The synthesis of **1a–e** was accomplished reacting diaminomaleonitrile with an  $\alpha$ -diketone in glacial acetic acid as the solvent (Figures S4–S6).<sup>17</sup>

According to a modified procedure reported by Donzello et al. and Renzi and co-workers, pyrazinoporphyrazine macrocycles **2a–e**<sup>18</sup> and titanium-based complexes of tetrakis-2,3-[5,6-di- $R_8$  pyrazino]porphyrazine<sup>19</sup> **3a–e** were obtained by autocyclotramerization of **1a–e** at high temperatures (from 180 to 250°C according to the precursor melting point) in the presence of a base or  $Ti(OBu)_4$ , respectively. In order to exclude  $O_2$  and avoid the presence of  $H_2O$ , complexes **3a–e** were synthesized applying Schlenk technique and stringent dry reaction conditions in the presence of an excess of **1a–e** (8 eq.). On the contrary, complex **4a** was obtained from stoichiometric amounts of starting material **1a** and an excess of  $Ti(OBu)_4$  (1.5 eq.) (Figure S21). In both cases, the work up procedure consisted in washing the greenish/bluish solids **3a–e/4a** with MeOH and/or  $CH_2Cl_2$ , followed by centrifugation and drying to constant weight under vacuum.

Thermogravimetric analysis and SEM micrographs of complexes **3a** and **4a** were also realized and included as Supporting Information (Figures S23–S27).

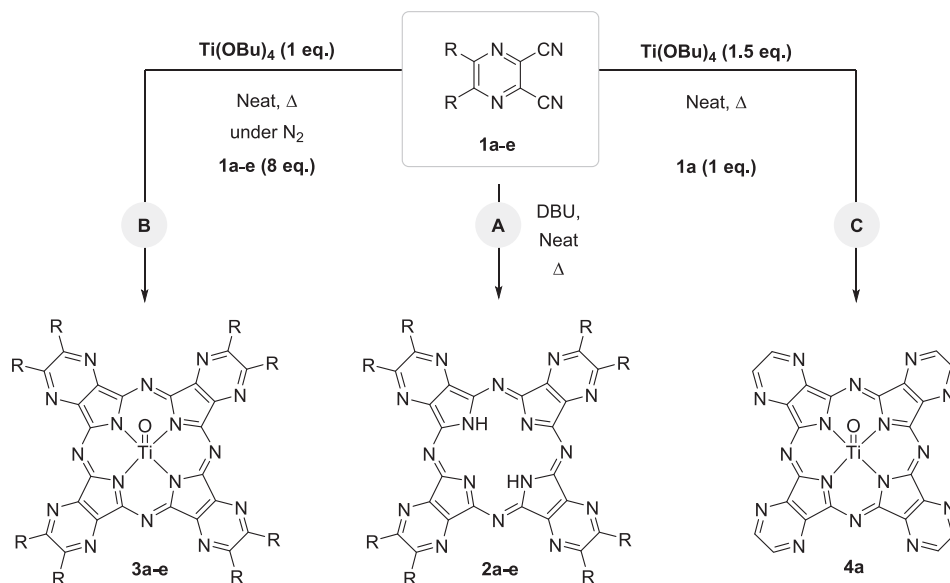
### 2.2 | Electrochemical characterization

Cyclic voltammetry (CV) experiments were performed at room temperature with a standard electrochemical setup, composed of a computer-controlled potentiostat, AUTOLAB PGSTAT12. The electrochemical cell was a conventional three-electrode cell with:

- Electrodes: glassy carbon disc 5 mm diameter (working electrode), rotating ring-disc electrode (RRDE) with glassy carbon disc 5 mm diameter and Pt ring (working

**SCHEME 1** Reaction scheme for the synthesis of ligands **2a–e** and titanium-based complexes of tetrakis-2,3-[5,6-di-R<sub>8</sub> pyrazino]porphyrazine—R = (a) H, (b) 2-Py, (c) Ph, (d) 4-MeOPh and (e) 4-BrPh—with (**4a**) and without (**3a–e**) the excess of Ti (OBU)<sub>4</sub>.

Reaction conditions: (A) **1a–e** (3.1 mmol), DBU few drops; (B) **1a–e** (3.1 mmol, 8 eq.), Ti (OBU)<sub>4</sub> (0.39 mmol, 1 eq.); (C) **1a** (3.1 mmol, 1 eq.), Ti (OBU)<sub>4</sub> (4.65 mmol, 1.5 eq.).



R = a) H, b) 2-Py, c) Ph, d) 4-MeOPh, e) 4-BrPh

electrode in RRDE experiments), glassy carbon rod (counter electrode), Ag/AgCl/NET<sub>4</sub>Cl 0.1 M in acetonitrile (reference electrode). Considering the non-aqueous electrolyte employed, the redox couple ferrocene/ferrocenium can be employed as an additional reference. In our conditions, 0.40 M HCl and in 0.40 M H<sub>2</sub>SO<sub>4</sub> in DMSO, the ferrocene/ferrocenium redox couple is, respectively, 475 mV and 465 mV more positive than the reference electrode Ag/AgCl/NET<sub>4</sub>Cl.

- Electrolyte: 0.40 M TfOH, or HCl, or H<sub>2</sub>SO<sub>4</sub> in DMSO;
- Scan Rates: 10, 50, 100 and 200 mV s<sup>-1</sup>;
- N<sub>2</sub> or O<sub>2</sub> atmosphere, with continuous gas flow of 100 mL min<sup>-1</sup>.

Exhaustive chronoamperometries were carried out on a glassy carbon plate electrode with 10 cm<sup>2</sup> of active surface.

Rotating ring disk (RRDE) experiments were performed at room temperature using a standard three-electrode glass cell with a Metrohm Autolab PGSTAT302N potentiostat and a Metrohm RRDE rotator. A Metrohm RRDE tip (RRDE Pt-GC) with a glassy carbon disc 5 mm diameter and a Pt ring was used as working electrode. Ag/AgCl/KCl (3 M) and a Pt sheet were employed as reference electrode and counter electrode, respectively. Prior to each experiment, the electrolyte, 0.1 M H<sub>2</sub>SO<sub>4</sub> in DMSO, was saturated with a gas flow of synthetic air (80% N<sub>2</sub>/20% O<sub>2</sub>) for 30 min at 100 sccm min<sup>-1</sup>. The measurements were executed by sweeping the electrode potential between 0.4 V and -1.25 V versus Ag/AgCl at a scan rate of 100 mV s<sup>-1</sup> with a ring potential of 1.2 V versus Ag/AgCl. Rotation

rates of 0, 100, 200, 400, 800, 1600 and 3200 rpm were applied while the gas flow was stopped. All the additional CV experiments, not been included in the manuscript, are reported in the Supporting Information (see Figures S28–S44).

### 3 | RESULTS AND DISCUSSION

As shown previously in the literature,<sup>19</sup> titanium complexes **3a–c** showed in DMSO or DMF five different redox events involving both the metal centre and the TPyzPzs macrocycle reductions. Therefore, in order to exploit these redox features, we became interested in a possible application of these complexes in ORR processes. In order to understand their redox behaviour in acidic conditions, CV measurements were first carried out under N<sub>2</sub> atmosphere. In these conditions, we were able to assess the activation potential of the titanium-complexes **3a–e**, if they can be reduced or oxidized and if their redox reactions are reversible. The same experiments were repeated under O<sub>2</sub> atmosphere to assess their electrochemical activity towards ORR. In particular, cathodic currents below 0.25 V versus Ag/AgCl could imply ORR activity. Those currents must be larger than under N<sub>2</sub>-purged electrolyte to be assigned to the ORR by the complex. In addition, considering that glassy carbon electrodes can reduce molecular O<sub>2</sub> to H<sub>2</sub>O<sub>2</sub>, blank experiments must be carried out. Therefore, the complex, to be considered active for ORR, should also yield larger currents under O<sub>2</sub> atmosphere than blank experiments.

To have a complete picture of the redox behaviour of complexes **3a–e**, we explored a potential window between  $-1$  V and  $+1$  V versus Ag/AgCl. Moreover, CVs were performed at several scan rates to investigate the different electrochemical processes which can occur at the electrode. Low scan rates allow the easier recognition of diffusion limiting currents and the assessment of the contribution of the Faradaic current. Conversely, capacitive current becomes predominant at faster scan rates. In general, we did not observe dramatic changes among the various scan rates explored. The main differences were found in the interval  $0/+1$  V versus Ag/AgCl, especially in the anodic scan direction, because of the almost complete lack of Faradaic contributions in that region. CVs highlighted the Faradaic processes occurring at the electrolyte/electrode interface.

In this first set of experiments, the potential window explored was quite narrow, but sufficient to show the activity towards  $O_2$  reduction at potential values lower than  $0.25$  V versus Ag/AgCl.

In order to understand the catalytic role played by the ligand and by the metal, the first electrochemical measurements were performed on compounds **2a–e**. All the five ligands, independently from their substitution pattern and the acidic electrolyte nature (TfOH, HCl or  $H_2SO_4$ ), did not show significant new current features compared with blank experiments with and without  $O_2$ . Their CVs were superimposable—within experimental error—to those of acidic DMSO which was employed as the electrolyte (Figures 1 and S1–S4 for TfOH, Figures S10–S14 for HCl and Figures S22–S26 for  $H_2SO_4$ ). Only in the case of ligand **2a**, we observed a 10% and a

25% current increase in HCl and  $H_2SO_4$ , respectively, at  $-0.5$  V versus Ag/AgCl, where the glassy carbon working electrode itself becomes active towards ORR (Figures S10b and S21). Under  $N_2$  atmosphere, the lack of redox features witnessed the unfeasibility of ligands oxidation or reduction in the wide potential window explored. Therefore, we concluded that macrocycles **2a–e** are very stable in the experimental conditions and not able to promote any catalytic reaction in the presence of  $O_2$ . Any catalytic activity that will be later demonstrated by the complexes would be thus ascribed to the presence of the titanium metal centre. Consequently, we started to investigate the redox behaviour of the titanium-based TPyzPzs **3a–e**.

Under  $N_2$  atmosphere, the simpler complex **3a** demonstrated significant cathodic current increase below  $0.2$  V versus Ag/AgCl. The complex has therefore redox states at those potential values and can be reversibly reduced at  $+0.2$  V and irreversibly reduced at  $-0.2$  V in DMSO in the presence of TfOH  $0.4$  M (Figure 2a). As the cathodic current increased three times passing from  $N_2$ -purged electrolyte to  $O_2$ -saturated conditions (Figures 2b and S5), we can state that the irreversible reduction is active for the reduction of  $O_2$ . Since we were not able to observe any current increase for the corresponding ligand **2a**, we can conclude that the catalytic activity displayed under  $O_2$  is due to the presence of the metal centre. The introduction of substituents on the macrocycle framework (e.g., 2-pyridyl, phenyl, 4-methoxyphenyl and 4-bromophenyl groups) is not beneficial for the ORR activity; in fact, complexes **3b–e** did not show any current growth compared to the blank in the same conditions

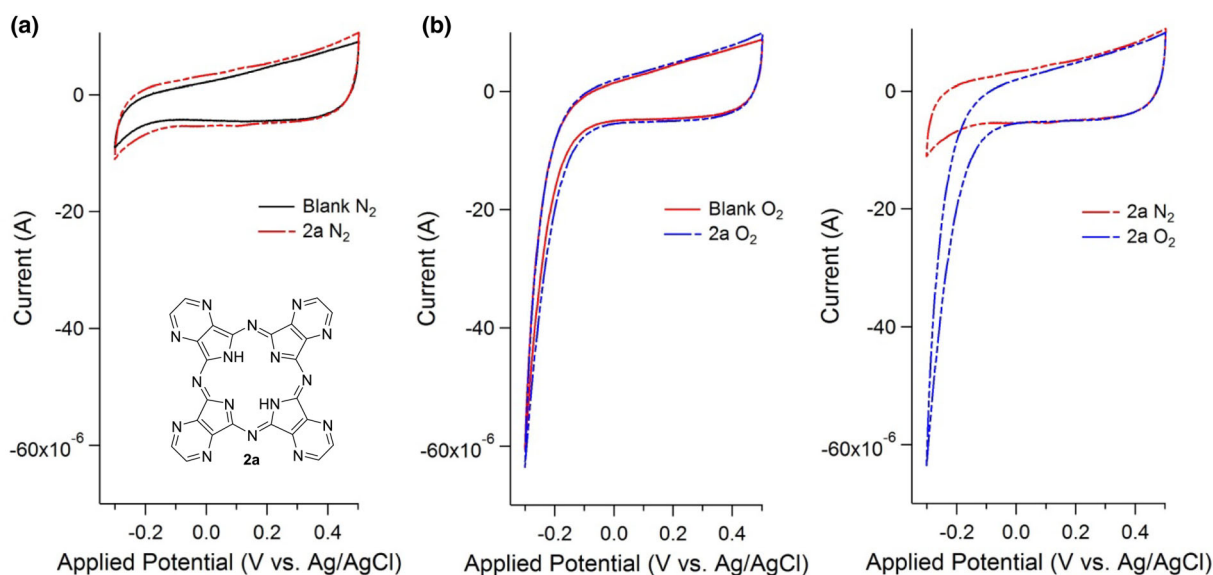
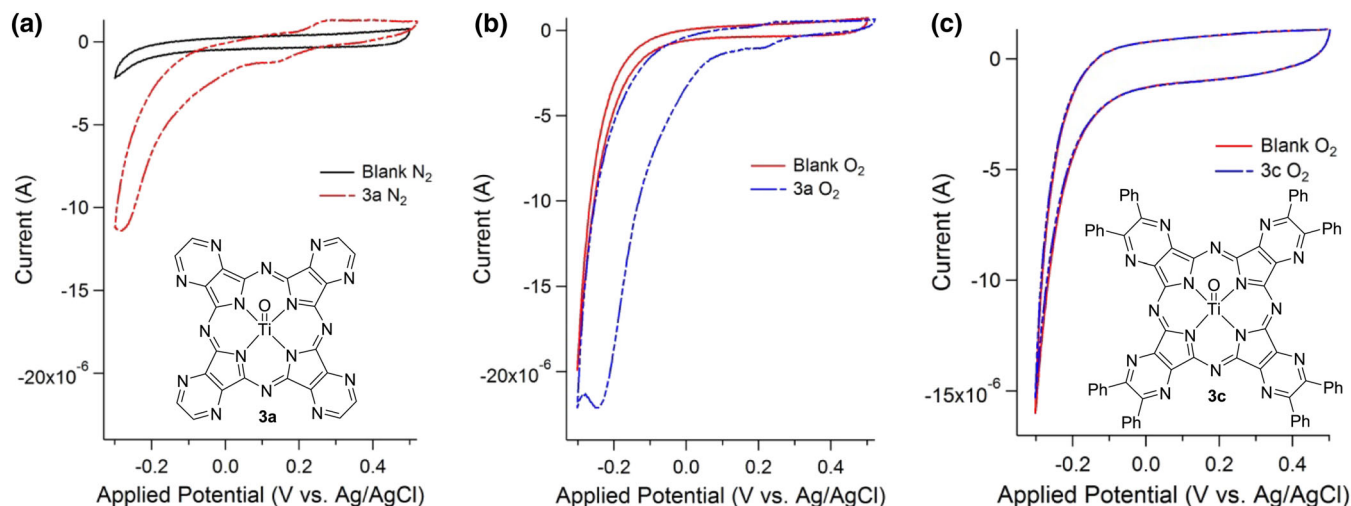


FIGURE 1 CV of 0.2 mM ligand **2a** in (a)  $N_2$ -purged 0.40 M TfOH in DMSO compared with blank experiment; (b)  $O_2$ -purged 0.40 M TfOH in DMSO compared with blank experiment; (c)  $N_2$ - and  $O_2$ -purged 0.40 M TfOH in DMSO. Potential scan rate  $100$   $mV s^{-1}$ .



**FIGURE 2** (a) CV of 0.2 mM complex **3a** in  $N_2$ -purged 0.40 M TfOH in DMSO compared with blank experiment; (b) CV of the complex **3a** in  $O_2$ -purged 0.40 M TfOH in DMSO compared with blank experiment; (c) CV of the complex **3c** in  $O_2$ -purged 0.40 M TfOH in DMSO compared with blank experiment. Scan rate  $100 \text{ mV s}^{-1}$ .

(Figures 2c and S6–S9). In addition, the current increase at potential values more negative than  $-0.25 \text{ V}$  (cathodic current peak at  $-0.45 \text{ V}$  vs. Ag/AgCl, vide infra), which is present in all the CVs in  $O_2$ -containing electrolytes, was assigned to the ORR process on glassy carbon.

To understand if the acid's conjugated base was playing any role in the ORR process, we investigated the electrochemical activity of **3a–e** under  $O_2$  in the presence of HCl and  $H_2SO_4$  0.4 M always employing DMSO as the solvent. To better characterize the compounds under investigation, the CVs in the  $O_2$ -saturated electrolyte were recorded with a broader potential window. Employing HCl instead of TfOH, no significant difference was observed. Only the complex **3a** showed a marginal larger current in the potential range 0–0.2 V versus Ag/AgCl with a perceivable loss of reversibility in the presence of HCl (Figures 3b and S15). Below 0 V versus Ag/AgCl, the current values recorded were very similar with either TfOH or HCl (Figure 3c). Substituted complexes **3b–e** confirmed to be inactive also in these conditions, not showing significant differences compared with the blank measurements (Figures S16–S19). Similar results were obtained with  $H_2SO_4$ , with only negligible displacements in the potentials (Figures 4 and S27–S30).

Interestingly complex **4a**, which was synthesized following a different procedure compared to electrocatalyst **3a**, also demonstrated activity towards the reduction of  $O_2$  (Figures 3d, S20, S31 and S32), showing a redox feature at  $-0.25 \text{ V}$ . It is, therefore, active for ORR in both HCl and  $H_2SO_4$  at potential values less negative than the ORR in blank electrolyte, occurring at  $-0.5 \text{ V}$ . The potential values at which **3a** and **4a** can reduce  $O_2$  are very similar; nevertheless, **4a** displays lower current values

compared with **3a**, witnessing sluggish kinetics compared to complex **3a**.

In order to gain insights into the selectivity of the  $O_2$  reduction for complexes **3a** and **4a**, RRDE experiments were performed. The potential of the disk electrode was scanned while the ring electrode was kept at  $+1.2 \text{ V}$  versus Ag/AgCl to oxidize back to  $O_2$  the  $H_2O_2$  possibly formed at the disc electrode. Therefore, if a 4-electron mechanism is operating, there will be no current at the ring electrode; conversely, if  $H_2O_2$  is produced through a 2-electron reduction, there will be anodic current at the ring electrode. Therefore, RRDE experiments allowed us to shed light on the ORR mechanism, as the possible formation of  $H_2O_2$  via 2-electron reduction could be promptly recorded at the ring electrode, because of the acquisition of an anodic current. Moreover, the current density at the ring electrode depends both on the amount of  $H_2O_2$  produced at the disc electrode and on the collection efficiency of the ring electrode itself. Employing hexacyanoferrate (III) reduction as reference reaction (the latter is known to be reduced with 100% Faradaic efficiency),<sup>20</sup> we were able to calculate a collection efficiency CE of 0.42 for the ring electrode, calculated as (3):

$$CE = \left| \frac{i_R n_R}{i_D n_D} \right| \quad (3)$$

where  $i_R$  and  $i_D$  are the currents recorded at the ring and disc electrodes, respectively, and  $n_R$  and  $n_D$  the electron transferred in disc and ring reactions, respectively. For hexacyanoferrate (III),  $n_R = n_D = 1$ . In the case of the blank experiment, without any complex in solution, ORR is carried out through 2-electron transfer at the GCE disc,

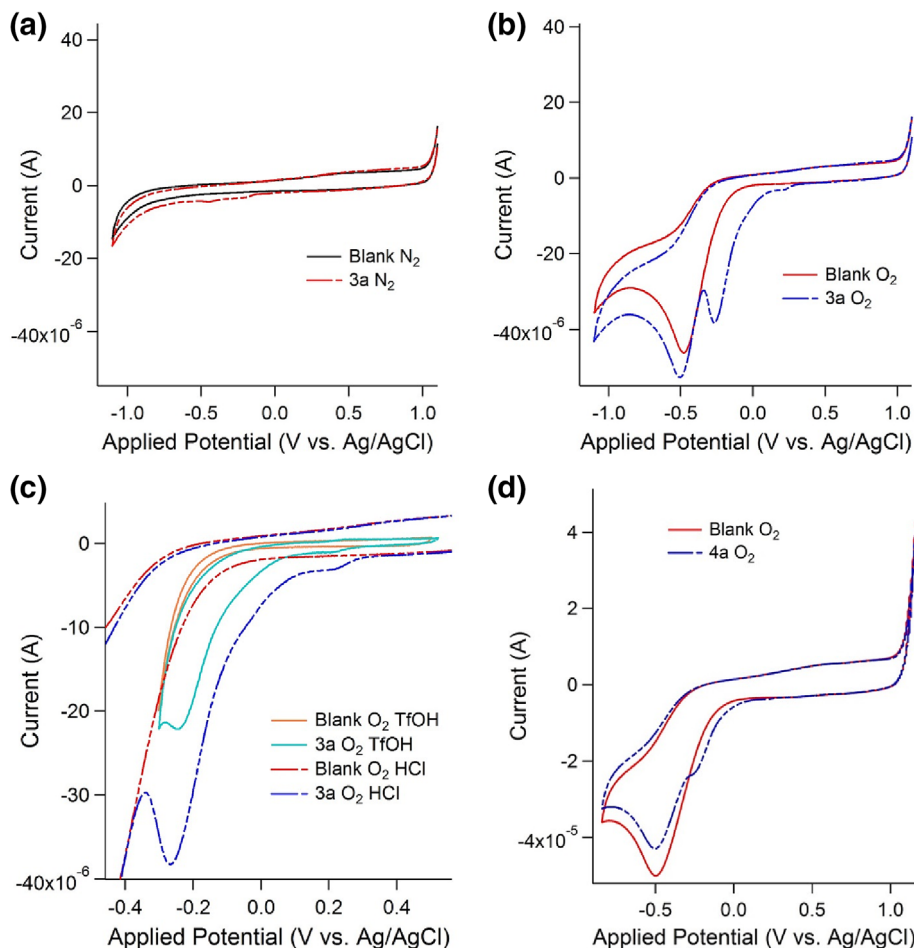


**FIGURE 3** (a) CV of 0.2 mM complex **3a** in N<sub>2</sub>-purged 0.40 M HCl in DMSO compared with blank experiment; (b) CV of 0.2 mM complex **3a** in O<sub>2</sub>-purged 0.40 M HCl in DMSO compared with blank experiment; (c) Comparison of the CVs of the blank and of 0.2 mM complex **3a** in O<sub>2</sub>-purged solution of DMSO in the presence of 0.40 M HCl or TFOH. Enlargement of the potential window between  $-0.6$  V/  $+0.5$  V. Scan rate  $100 \text{ mV s}^{-1}$ ; (d) CV of 0.2 mM complex **4a** in O<sub>2</sub>-purged 0.40 M HCl in DMSO compared with blank experiment.

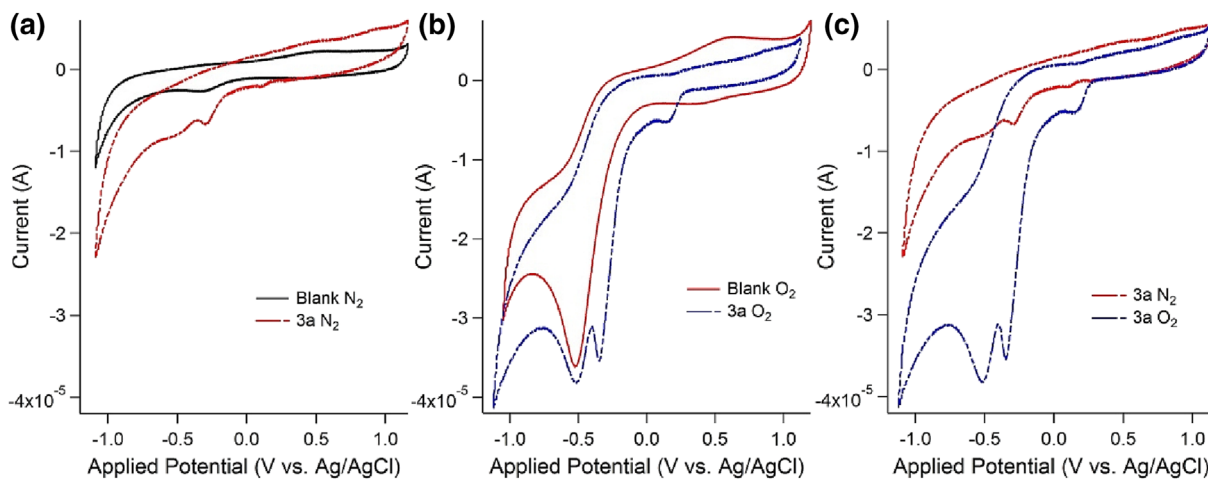
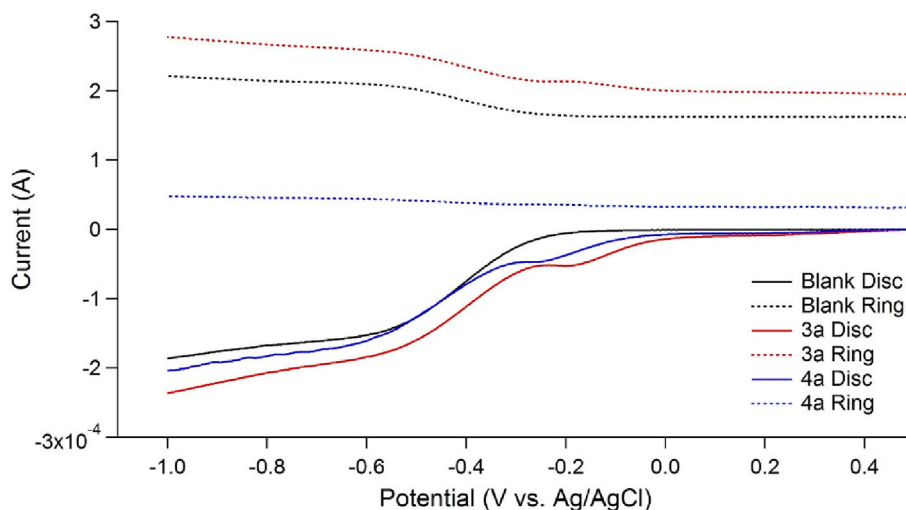


**FIGURE 4** (a) CV of 0.2 mM electrocatalyst **3a** in N<sub>2</sub>-purged 0.40 M H<sub>2</sub>SO<sub>4</sub> in DMSO compared with blank experiment; (b) CV of the complex **3a** in O<sub>2</sub>-purged 0.40 M H<sub>2</sub>SO<sub>4</sub> in DMSO compared with blank experiment; (c) comparison between the CV measurements in N<sub>2</sub>- and O<sub>2</sub>-purged 0.40 M H<sub>2</sub>SO<sub>4</sub> in DMSO for Ti-complex **3a**. Scan rate  $100 \text{ mV s}^{-1}$ .

producing mainly H<sub>2</sub>O<sub>2</sub>. In our conditions, we were able to observe at the ring electrode at 1000 rpm and  $-1.0$  V versus Ag/AgCl a recovery of H<sub>2</sub>O<sub>2</sub> of 0.35, which is slightly lower than the value found in the case of

potassium ferricyanide (0.42), confirming that GCE is mainly active in H<sub>2</sub>O<sub>2</sub> formation.<sup>3a</sup> In the case of the complex **3a**, we observed a significant cathodic current increase at the disc electrode, coherently with the former

**FIGURE 5** LSV recorded at RRDE at 1000 rpm of 0.2 mM complexes **3a** and **4a** in O<sub>2</sub>-purged 0.1 M H<sub>2</sub>SO<sub>4</sub> in DMSO compared with the blank experiment.



measurements, especially in the potential range from 0 to  $-0.4$  V versus Ag/AgCl (Figure 5). Additionally, we observed a H<sub>2</sub>O<sub>2</sub> collection efficiency around 0.34 at the ring electrode, very close to the blank value, witnessing that, even if the complex **3a** is capable of improving activity compared with the blank, the mechanism involves the transfer of 2-electron to form almost exclusively H<sub>2</sub>O<sub>2</sub>. Based on the RRDE experiment, we can conclude that 82%, for the blank, and 81%, for the complex **3a**, of the transferred electrons contribute to the production of H<sub>2</sub>O<sub>2</sub>.

Conversely, in the case of complex **4a**, we noticed a different behaviour: at the disc electrode, we observed very similar current densities compared with the complex **3a**, evidencing activity toward ORR, but with significantly lower current values at the ring electrode (Figure 5, collection efficiency of 0.13), implying that the ORR proceeds mainly with a 4-electron path, with  $\approx 70\%$  of transferred electrons concurring to H<sub>2</sub>O formation from O<sub>2</sub>.

Finally, to demonstrate that titanium-based complexes **3a** and **4a** have a real catalytic activity toward ORR and exclude that these compounds were merely acting as reactants in the electrolyte (Figure S32), we performed exhaustive chronoamperometries (see Figure S45). If the compounds would have act as mere reactants, the current had dropped to the blank value once the reactants will be consumed (i.e., a TON  $\approx 1$ ). Conversely, if the compounds behave as catalysts, then a TON  $> 1$  will be achieved. To avoid the participation of the glassy carbon electrode to the ORR process, we recorded chronoamperometries at the potential of the first O<sub>2</sub> reduction ( $-0.200$  V vs. Ag/AgCl) for 4 h. In the case of complex **3a**, the current values recorded were close to those observed in the CV ( $0.4 \div 0.5$  mA) and tended to slightly decrease with time, reaching  $50 \div 60\%$

of the initial current after 2 h and  $40 \div 50\%$  after 4 h. Assuming a faradaic efficiency of 100% for 2-electron ORR, we calculated a TON of 4.5 for complex **3a** in 0.40 M HCl in DMSO, demonstrating a catalytic activity for **3a** towards the formation of H<sub>2</sub>O<sub>2</sub>.

In the case of complex **4a**, we observed current densities in the order of 0.3 mA with more constant behaviour over time. More than 80% or 70% of the initial current was retained respectively after 2 or 4 h. Again, TONs were larger than 1, reaching the value of 4.4 considering a 2-electron ORR or 2.2 in the case of 4-electron ORR, the latter being the main reaction path for this complex, as evidenced by RRDE experiments (Figure S32). As recently summarized in different papers,<sup>9a,21</sup> homogeneous catalysts for H<sub>2</sub>O<sub>2</sub> production are mainly transition metal-complexes bearing Co, Mn, Fe or Cu generally employed in aqueous solution or in organic solvents different from DMSO. Therefore, a direct comparison with the results obtained with compounds **3a** and **4a** cannot be realized.

## 4 | CONCLUSION

In the present work, we demonstrated the application of titanium-based TPyzPzs as electrocatalysts in the ORR process. Between the different TPyzPzs ligands and the corresponding Ti = O complexes synthesized, only the unsubstituted complex **3a** showed electrocatalytic activity toward ORR proving a deactivating effect caused by the introduction of 2-Py, Ph, 4-MeOPh and 4-BrPh substituents on the macrocyclic core. A change in the synthetic conditions and the usage of an excess of the titanium precursor delivered complex **4a** showing a certain activity for ORR too. It is interesting to notice that no homogeneous catalysts bearing titanium as the metal-centre have

been reported so far, notwithstanding its moderate affinity for peroxide has been known since decades. Our electrocatalytic measurements confirmed the O<sub>2</sub> reduction activity as an emerging property of the complex, as the ligand **2a** alone was not active in ORR. Moreover, RRDE experiments allowed us to assess the main mechanisms and reduction products in the ORR process promoted by **3a** and **4a**. While complex **3a** mainly produces H<sub>2</sub>O<sub>2</sub>, with complex **4a**, the 4-electron reduction is the preferred reaction path. Bulk electrolysis confirmed **3a** and **4a** to be real catalysts reaching TONs larger than 4 considering 2-electron reduction products. The introduction of other non-noble metals in TPyzPzs for ORR is currently under evaluation.

## AUTHOR CONTRIBUTIONS

**Fabrizio Sordello**: Conceptualization; investigation; funding acquisition; writing—original draft. **Pelagia-Nefeli Prantsidou-Georgiadou**: Investigation. **Emanuele Azzi**: Investigation. **Yannick Tschauder**: Investigation. **Dario Formenti**: Investigation. **Francesco Pellegrino**: Investigation; funding acquisition; writing—original draft. **Polyssena Renzi**: Conceptualization; investigation; funding acquisition; project administration; writing—original draft. All authors reviewed the paper.

## ACKNOWLEDGEMENTS

We thank Mrs Birgit Hahn (RWTH Aachen University) for SEM/EDX analysis and Mrs Anne Frommelius (RWTH Aachen University) for TGA analysis. We thank Fondazione CRT-Cassa di Risparmio di Torino for financial support.

## CONFLICT OF INTEREST STATEMENT


The authors declare no conflict of interest.

## DATA AVAILABILITY STATEMENT


Data available on request from the authors.

## ORCID

**Fabrizio Sordello**  <https://orcid.org/0000-0003-4578-2694>

**Pelagia-Nefeli Prantsidou-Georgiadou**  <https://orcid.org/0009-0006-6780-3010>

**Emanuele Azzi**  <https://orcid.org/0000-0002-2284-2925>

**Yannick Tschauder**  <https://orcid.org/0000-0002-2417-1854>

**Dario Formenti**  <https://orcid.org/0000-0003-1603-4179>

**Francesco Pellegrino**  <https://orcid.org/0000-0001-6126-0904>

**Polyssena Renzi**  <https://orcid.org/0000-0002-1326-8183>

## REFERENCES

- [1] a) Y. Pang, H. Xie, Y. Sun, M.-M. Titirici, G.-L. Chai, *J. Mat. Chem. A* **2020**, *8*, 24996; b) N. Wang, S. Ma, P. Zuo, J. Duan, B. Hou, *Adv. Sci.* **2021**, *8*, 2100076.
- [2] C. A. Martínez-Huitle, S. Ferro, *Chem. Soc. Rev.* **2006**, *35*, 1324.
- [3] a) E. Brillas, I. Sirés, M. A. Oturan, *Chem. Rev.* **2009**, *109*, 6570; b) R. Hage, A. Lienke, *Angew. Chem. Int. Ed.* **2006**, *45*, 206.
- [4] I. Yamanaka, T. Onizawa, S. Takenaka, K. Otsuka, *Angew. Chem., Int. Ed.* **2003**, *42*, 3653.
- [5] M. Melchionna, P. Fornasiero, M. Prato, *Adv. Mater.* **2019**, *31*, 1802920.
- [6] Y. Jiang, P. Ni, C. Chen, Y. Lu, P. Yang, B. Kong, A. Fisher, X. Wang, *Adv. Energy Mater.* **2018**, *8*, 1801909.
- [7] J. M. Campos-Martin, G. Blanco-Brieva, J. L. G. Fierro, *Angew. Chem., Int. Ed.* **2006**, *45*, 6962.
- [8] a) S. Siahrostami, A. Verdaguer-Casadevall, M. Karamad, D. Deiana, P. Malacrida, B. Wickman, M. Escudero-Escribano, E. A. Paoli, R. Frydendal, T. W. Hansen, I. Chorkendorff, I. E. L. Stephens, J. Rossmeisl, *Nat. Mater.* **2013**, *12*, 1137; b) A. Verdaguer-Casadevall, D. Deiana, M. Karamad, S. Siahrostami, P. Malacrida, T. W. Hansen, J. Rossmeisl, I. Chorkendorff, I. E. L. Stephens, *Nano Lett.* **2014**, *14*, 1603; c) J. S. Jirkovský, I. Panas, E. Ahlberg, M. Halasa, S. Romani, D. J. Schiffrin, *J. Am. Chem. Soc.* **2011**, *133*, 19432; d) X. Zhao, H. Yang, J. Xu, T. Cheng, Y. Li, *ACS Mater. Lett.* **2021**, *3*, 996.
- [9] a) Z. Liang, H.-Y. Wang, H. Zheng, W. Zhang, R. Cao, *Chem. Soc. Rev.* **2021**, *50*, 2540; b) S. Siahrostami, S. J. Villegas, A. H. B. Mostaghimi, S. Back, A. B. Farimani, H. Wang, K. A. Persson, J. Montoya, *ACS Catal.* **2020**, *10*, 7495; c) Y. Sun, L. Silvioli, N. R. Sahaie, W. Ju, J. Li, A. Zitolo, S. Li, A. Bagger, L. Arnarson, X. Wang, T. Moeller, D. Bernsmeier, J. Rossmeisl, F. Jaouen, P. Strasser, *J. Am. Chem. Soc.* **2019**, *141*, 12372; d) E. Jung, H. Shin, B.-H. Lee, V. Efremov, S. Lee, H. S. Lee, J. Kim, W. H. Antink, S. Park, K.-S. Lee, S.-P. Cho, J. S. Yoo, Y.-E. Sung, T. Hyeon, *Nat. Mater.* **2020**, *19*, 436.
- [10] a) Y.-H. Wang, B. Mondal, S. S. Stahl, *ACS Catal.* **2020**, *10*, 12031; b) A. B. Sorokin, *Chem. Rev.* **2013**, *113*, 8152; c) S. Huang, K. Chen, T.-T. Li, *Chem. Rev.* **2022**, *464*, 214563; d) Y. Tong, L. Wang, F. Hou, S. X. Dou, J. Liang, *Electrochem. Energy Rev.* **2022**, *5*, 7.
- [11] R. Jasinski, *Nature* **1964**, *201*, 1212.
- [12] a) W. Zhang, W. Lai, R. Cao, *Chem. Rev.* **2017**, *117*, 3717; b) Y. Nie, L. Li, Z. Wei, *Chem. Soc. Rev.* **2015**, *44*, 2168.
- [13] X. Zhao, Q. Yin, X. Mao, C. Cheng, L. Zhang, L. Wang, T.-F. Liu, Y. Li, Y. Li, *Nat. Commun.* **2022**, *13*, 2721.
- [14] a) B. D. Matson, C. T. Carver, A. Von Ruden, J. Y. Yang, S. Raugei, J. M. Mayer, *Chem. Commun.* **2012**, *48*, 11100; b) B. Sun, Z. Ou, S. Yang, D. Meng, G. Lu, Y. Fang, K. M. Kadish, *Dalton Trans.* **2014**, *43*, 10809; c) L. L. Chng, C. J. Chang, D. G. Nocera, *Org. Lett.* **2003**, *5*, 2421.
- [15] a) V. Novakova, M. P. Donzello, C. Ercolani, P. Zimcik, P. A. Stuzhin, *Coord. Chem. Rev.* **2018**, *361*, 1; b) M. P. Donzello, C. Ercolani, V. Novakova, P. Zimcik, P. A. Stuzhin, *Coord. Chem. Rev.* **2016**, *309*, 107.
- [16] a) S. Dong, B. Liu, J. Liu, N. Kobayashi, *J. Porphyr. Phthalocyanines* **1997**, *1*, 333; b) Z. Xu, H. Li, G. Cao, Q. Zhang, K. Li, X. Zhao, *J. Mol. Catal. A: Chem.* **2011**, *335*, 89; c) T. Hayashi, A.



- Ishihara, T. Nagai, M. Arao, H. Imai, Y. Kohno, K. Matsuzawa, S. Mitsushima, K.-i. Ota, *Electrochim. Acta* **2016**, *209*, 1.
- [17] E. H. Mørkved, H. Ossletten, H. Kjøen, O. Bjørlo, *J. Prakt. Chem.* **2000**, *342*, 83.
- [18] a) M. P. Donzello, Z. Ou, D. Dini, M. Meneghetti, C. Ercolani, K. M. Kadish, *Inorg. Chem.* **2004**, *43*, 8637; b) M. P. Donzello, Z. Ou, F. Monacelli, G. Ricciardi, C. Rizzoli, C. Ercolani, K. M. Kadish, *Inorg. Chem.* **2004**, *43*, 8626.
- [19] P. Renzi, L. Mazzapioda, F. Nardelli, F. Martini, M. Geppi, C. Mancone, M. Assunta Navarra, F. D'Acunzo, P. Gentili, *Eur. J. Inorg. Chem.* **2020**, *2020*, 2417.
- [20] U. A. Paulus, T. J. Schmidt, H. A. Gasteiger, R. J. Behm, *J. Electroanal. Chem.* **2001**, *495*, 134.
- [21] a) S. Yang, Y. Yu, X. Gao, Z. Zhang, F. Wang, *Chem. Soc. Rev.* **2021**, *50*, 12985; b) J. Han, N. Wang, X. Li, W. Zhang, R. Cao, *J. Phys. Chem. C* **2021**, *125*, 24805; c) Y. Wang, G. I. N.

Waterhouse, L. Shang, T. Zhang, *Adv. Energy Mater.* **2021**, *11*, 2003323.

## SUPPORTING INFORMATION

Additional supporting information can be found online in the Supporting Information section at the end of this article.

**How to cite this article:** F. Sordello, P.-N. Prantsidou-Georgiadou, E. Azzi, Y. Tschauder, D. Formenti, F. Pellegrino, P. Renzi, *Appl Organomet Chem* **2023**, e7116. <https://doi.org/10.1002/aoc.7116>